Cannabinoids reveal importance of spike timing coordination in hippocampal function

David Robbe[1], Sean M Montgomery[1], Alexander Thome[2], Pavel E Rueda-Orozco[1], Bruce L McNaughton[2] & György Buzsaki[1]

Cannabinoids impair hippocampus-dependent memory in both humans and animals, but the network mechanisms responsible for this effect are unknown. Here we show that the cannabinoids Δ^9-tetrahydrocannabinol and CP55940 decreased the power of theta, gamma and ripple oscillations in the hippocampus of head-restrained and freely moving rats. These effects were blocked by a CB1 antagonist. The decrease in theta power correlated with memory impairment in a hippocampus-dependent task. By simultaneously recording from large populations of single units, we found that CP55940 severely disrupted the temporal coordination of cell assemblies in short time windows (< 100 ms) yet only marginally affected population firing rates of pyramidal cells and interneurons. The decreased power of local field potential oscillations correlated with reduced temporal synchrony but not with firing rate changes. We hypothesize that reduced spike timing coordination and the associated impairment of physiological oscillations are responsible for cannabinoid-induced memory deficits.

The primary psychoactive constituent of marijuana, delta-9-tetrahydrocannabinol (Δ^9-THC), binds to G-protein coupled CB1 receptors, which are expressed at high levels in the hippocampus, neocortex, cerebellum and basal ganglia[1,2]. In humans, Δ^9-THC affects working and episodic memories[3–5], the latter being dependent on hippocampal function[6]. In rats, both systemic and intrahippocampal injections of cannabinoids impair memory in hippocampus-dependent spatial and delayed nonmatch to sample tasks[7–9]. In vivo, Δ^9-THC reduces the power of local field potentials and electroencephalograms in various frequency bands in both the hippocampus and the neocortex[3,10–12] by hitherto unknown mechanisms. The involvement of intrahippocampal circuits has been suggested based on the observation that kainate-induced gamma oscillations are attenuated by CB1 receptor activation in vitro[13].

In the hippocampus, temporal coordination of excitatory and inhibitory synaptic potentials supports at least three types of network activity associated with the formation of hippocampus-dependent memories[14]. Hippocampal theta (4–12 Hz) and gamma (30–80 Hz) oscillations play a fundamental role in coordinating assembly firing across the hippocampo-prefrontal cortical regions[15] and are believed to be critical for working memory[16] and encoding episodic memories[17]. Ripple (100–200 Hz) oscillations, on the other hand, assist with long-term consolidation of the memory trace and transfer of hippocampal memories to neocortical stores[18,19]. Despite this information, it remains largely unknown how the coordination of hippocampal cell assemblies gives rise to these network patterns and supports mnemonic functions of the hippocampus.

Here, we show that cannabinoids disrupt the temporal coordination of hippocampal neurons and deteriorate theta, gamma and ripple network patterns without substantial changes in principle cell and interneuron average firing rates. Furthermore, we found that the reduction of hippocampal theta oscillations by cannabinoids correlates with memory impairment in a hippocampus-dependent task.

RESULTS

CB1 receptor activation decreased hippocampal oscillations

To examine the consequences of cannabinoids on the ensemble activity of the hippocampus, multiple single units and local field potentials were recorded from the CA1 pyramidal layer using two-dimensional silicon probes in head-restrained awake rats ($n = 4$, **Supplementary Methods** online). The CB1 receptor agonist CP55940 decreased the overall power of the local field potential (LFP) oscillations in a dose-dependent manner (**Fig. 1**, 0.03–0.3 mg per kg body weight)[3,10–12]. This effect was visible in the raw traces as a general 'flattening' of the LFP (**Fig. 1a**). The drug decreased the power of all three major oscillatory hippocampal patterns, mainly in the theta and fast ripple bands, with a less pronounced effect in the gamma frequency range (**Fig. 1b,c,e**). The agonist-induced decrease in the LFP power was dose dependent (**Fig. 1c,e**; dose effect $P = 0.0064$) and effectively blocked by pre-administration of the CB1 receptor antagonist (inverse agonist) SR141716A (**Fig. 1d,f**; CP55940 dose effect: $P = 0.33$), showing the receptor specificity of the effect. The antagonist SR141716A alone did not induce a significant effect on any measured aspect of network activity (**Supplementary Fig. 1** online).

[1]Center for Molecular and Behavioral Neuroscience, Rutgers, The State University of New Jersey, Newark, New Jersey 07102, USA. [2]Division of Neural Systems, Memory and Aging, University of Arizona, Tucson, Arizona 85724, USA. Correspondence should be addressed to G.B. (buzsaki@axon.rutgers.edu).
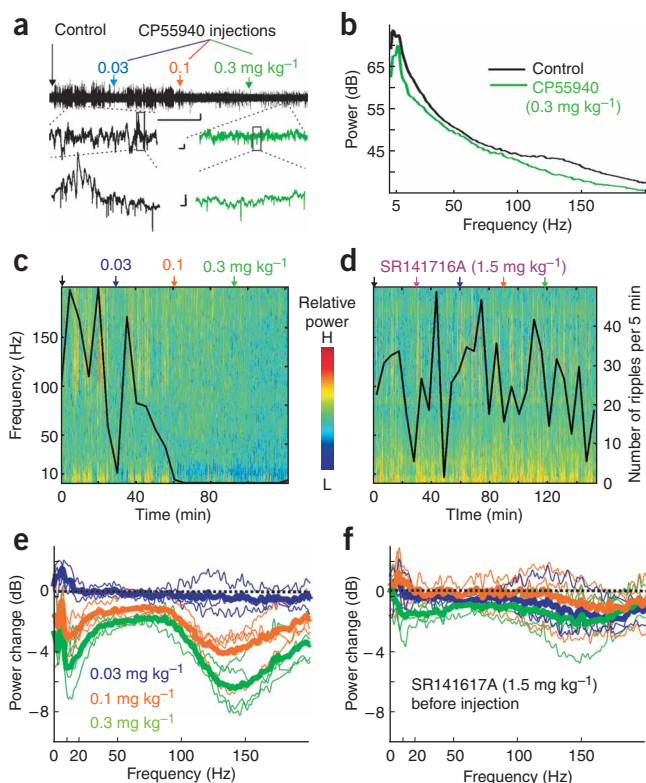
Figure 1 CB1 receptor activation decreases the power of the LFP oscillations. (**a**) Compressed wide-band recording of LFP (2 h). Insets, epochs with increasing time resolution reveal dynamic LFP patterns and single units. Scale bars (top-down), 20 min/0.5 mV, 150 ms/0.2 mV, 10 ms/0.2 mV. (**b**) Power spectra of respective segments in **a**. (**c**) Power spectrogram during the control condition and after increasing doses of CP55940. (**d**) Similar to **c** but the agonist application is preceded by injection of the CB1 inverse agonist SR141716A. Data from a single rat shown in **a**–**d**. (**e**,**f**) Group results, showing spectral differences from baseline. Thin lines, individual experiments; bold lines, mean for each drug condition.

## Reduction of LFP power correlates with memory impairment

In control conditions, head-restrained rats alternate between awake and sleep states and one can argue that CP55940 biases the behavioral state of the animal, accounting for the reduced power of field oscillations. However, CP55940 did not simply shift the behavioral state between the antagonistic theta/gamma and ripple network patterns, as both theta and ripple oscillations were affected (**Fig. 1b,c,e**). To further address this issue, we examined the effects of CP55940 (0.1–0.3 mg kg^{-1}) in additional rats ($n = 5$) trained to run on an elevated track, a behavior strongly associated with theta oscillations (**Fig. 2**, **Supplementary Methods**). Although the general motor activity (measured by running speed) of the animals was decreased after the

drug, locomotor changes could not account for the LFP changes (**Fig. 2a**). First, ripple power decreased despite the longer immobility periods (not shown). Second, the power of theta activity and its second harmonic was significantly lower after drug administration even when the effect of running speed was controlled by an analysis of covariance (**Fig. 2b**; ANCOVA $P < 0.001$ for each of 16 sessions from five rats). Four of the five rats were trained to perform a hippocampus-dependent delayed spatial alternation task (D.A. Ainge and E.R. Wood, *Soc. Neurosci. Abstr.* **91.1**, 2003 and **Supplementary Methods**). They were injected with the synthetic cannabinoid CP55940 and one, two or three behavioral sessions were recorded at various time intervals following the injection (range, 20 min to 4 h). The performance of the animal was compared to a control session carried out just before the injection. In agreement with previous studies, CP55940 significantly impaired the rats' performance in this hippocampus-dependent task[7–9] (**Fig. 2c**). To establish a link between behavioral performance and physiological parameters, we quantified the speed-corrected decrease in theta power (**Fig. 2c**, see Methods) between control and drug sessions. The reduction in theta power, brought about by CP55940, was significantly correlated with impairment in the delayed spatial alternation task performance (**Fig. 2d**).

Because CP55940 is a full CB1 agonist, whereas Δ^9-THC, the main psychoactive ingredient of marijuana, is a partial CB1-agonist, we examined whether the two compounds have a similar effect on hippocampal activity. Two additional animals were tested under the influence of Δ^9-THC (5 mg kg^{-1}), in their home cage and when running on an elevated circular track. Similar to the effects of CP55940, Δ^9-THC decreased the overall power of the LFP (1–250 Hz, **Fig. 3a**). During rest in the home cage, Δ^9-THC decreased the power in the ripple band and the incidence of ripple episodes ($P < 0.001$ in both
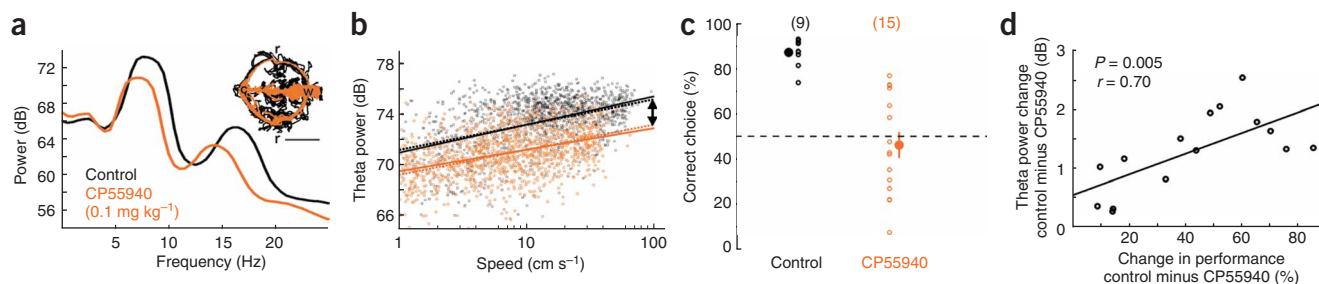
Figure 2 Cannabinoid-induced decrease of theta power is independent of locomotion speed of the rat and correlates with behavioral impairment in the hippocampus-dependent, delayed alternation memory task. (**a**) Power spectra of hippocampal LFP during control (black) and drug (0.1 mg kg^{-1} CP55940; red) conditions. Inset, locomotor path of a rat on the elevated track during a delayed alternation task in control (black) or after CP55940 (red). Scale bar, 1 m. w, waiting area; c, choice point; r, reward location. (**b**) Correlation between theta power and running speed (same experiment as in **a**). Note significantly lower power of theta during drug condition even at identical running speeds ($P < 0.001$). Solid lines, independent fit of slopes. Dashed lines, parallel fit of slopes. (**c**) Percentage of correct choices in control conditions (9 sessions, 4 rats) and after CP55940 (0.1–0.3 mg kg^{-1}, 15 sessions, 4 rats). One to three sessions were recorded at various intervals after CP55940 injection (range, 30 min to 4 h). Bold points represent mean ± s.e.m., $P < 0.001$. (**d**) Correlation between change in theta power (arrow in **b**, independent of speed change) and drug-induced decrease in behavioral accuracy during the alternation task ($n = 15$, 4 rats).
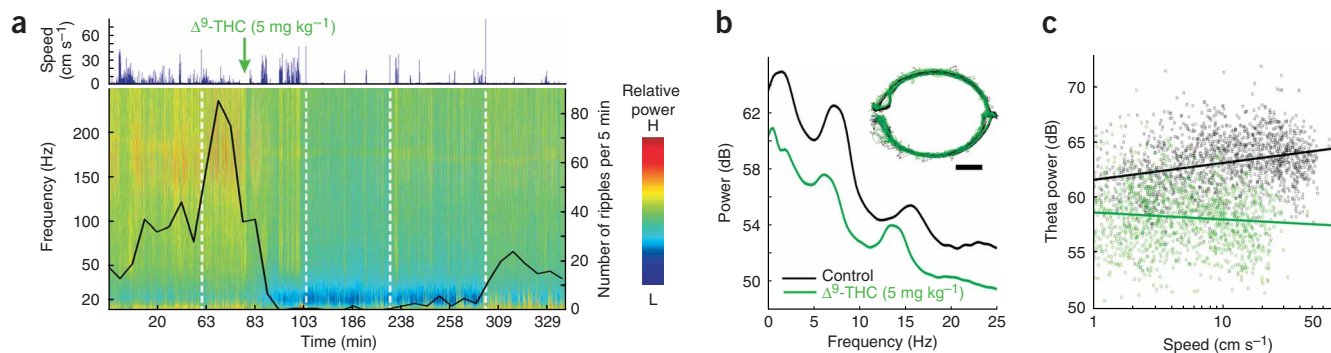
Figure 3 Δ^9-THC produces effects on LFP oscillations similar to CP55940. CA1 LFP was recorded in successive home cage (HC) and maze (M) sessions, (HC1-M1-HC2-M2-HC3-M3-HC4-M4-HC5). Δ^9-THC (5 mg kg^{-1}) was injected intraperitoneally (i.p.) in the middle of the second HC session. (**a**) Power spectrogram during the successive home cage sessions. The running line represents ripple incidence. Upper panel shows locomotor activity. (**b**) Power spectra of hippocampal LFP in control (black) and drug (Δ^9-THC, 5 mg kg^{-1}; green) conditions during maze running. Inset, locomotor path of the rat on the elevated track. Scale bar, 1 m. (**c**) Correlation between theta power and running speed. Note significantly lower power of theta during drug condition at identical running speeds ($P < 0.001$).

rats). This effect could not be explained by change in behavior because under the influence of Δ^9-THC, the animals showed longer immobility periods (**Fig. 3a** upper panel) that usually favor ripple occurrence. On the elevated track, both locomotor activity and the power of theta oscillations (**Fig. 3b,c**) were decreased by Δ^9-THC. Nevertheless, analysis of covariance revealed that the reduction of theta power was highly significant after controlling for effects of locomotion (**Fig. 3c**; $P < 0.001$; in both rats).

Effects of intrahippocampal injection of CP55940

To obtain further support for the hypothesis that the cannabinoids exerted effects directly on intrahippocampal circuits, we examined the consequences of CP55940 injected locally into the CA1 region (1 μg 0.5 μl^{-1} infused over 15 min) in three urethane-anesthetized rats. We chose to quantify the drug effect on ripple events because ripples are generated locally; their high frequency exhibits less volume conduction from nearby cell populations than lower frequency oscillations and they are generated independently in the two hemispheres[14,20,21]. To compensate for potential volume and osmotic effects, the drug and vehicle were infused simultaneously in separate hemispheres. In each hemisphere, LFPs were monitored in the CA1 pyramidal layer with four tungsten electrodes spaced 300 μm apart (**Fig. 4a**, inset). Because

preliminary experiments showed that local drug injection did not affect the LFP recorded at the most distant electrode (electrode 4; 1.2 mm from the injection site), we computed the ratio between ripple power at electrodes 2 and 4 in each hemisphere. This intra-animal design eliminated potential artifacts associated with sequential canula insertion and anesthesia-related state fluctuations of the brain.

Figure 4a illustrates ripple episodes before and after injection of CP55940 and vehicle. Quantitative comparison of the ripple power ratios (electrode 2/electrode 4) revealed a significant attenuation of ripple power by CP55940 versus vehicle injections (**Fig. 4**, $P < 0.001$ in each rat). As a further test to examine the effectiveness and local selectivity of volume infusion, at the end of each experiment a 10% solution of the local anesthetic lidocaine (0.5 μl) was infused in both sides. These control experiments verified that the commissurally evoked responses recorded by electrode 2 were powerfully reduced or eliminated while potentials recorded by electrode 4 remained essentially unchanged (**Fig. 4b**). Since the capacitive components of the extracellular medium and the cable properties of neurons strongly attenuate LFP fast frequency components (low-pass filtering), slow oscillations can spread through volume conduction more effectively than fast ones[22]. Therefore, the effect on theta and gamma oscillations was not examined because volume–conducted LFP from
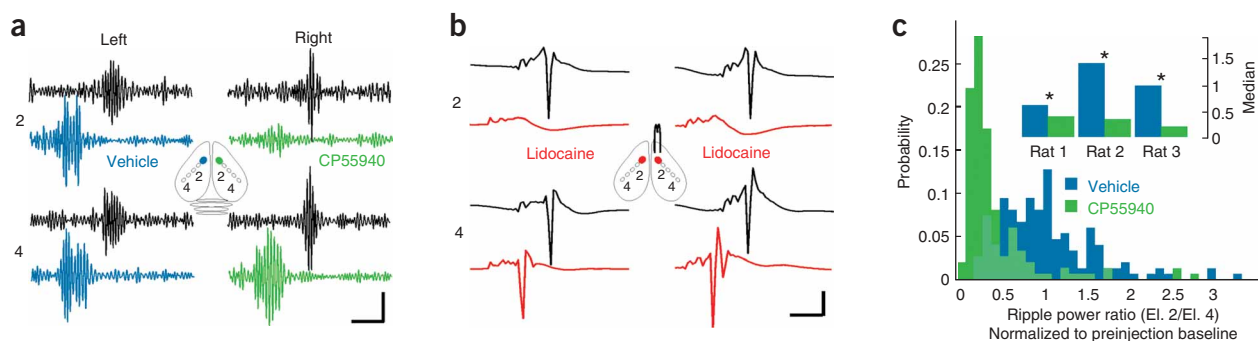
Figure 4 Intrahippocampal injection of CP55940 decreases ripple power. (**a**) 100–200 Hz filtered LFP traces showing simultaneously recorded ripples before (black traces) or after injection of 1 μg of CP55940 (green traces) or its vehicle (blue traces) in the right (R) and left (L) hippocampus. Inset, electrode arrangement relative to injection sites. Scale bars, 100 ms/0.15 mV. (**b**) Evoked response to commissural stimulation before (black) and 10 min after (red) injection of 500 nl of lidocaine (10%). Same experiment and recording sites as in **a**. Scale bars, 12 ms/2.5 mV. (**c**) Distribution of ripple power ratios (electrode 2/electrode 4 (El. 2/El. 4), $n = 149$ events in three rats; $n = 49/44/56$) after injection of vehicle and 1 μg of CP55940. Inset, median values for each rat.
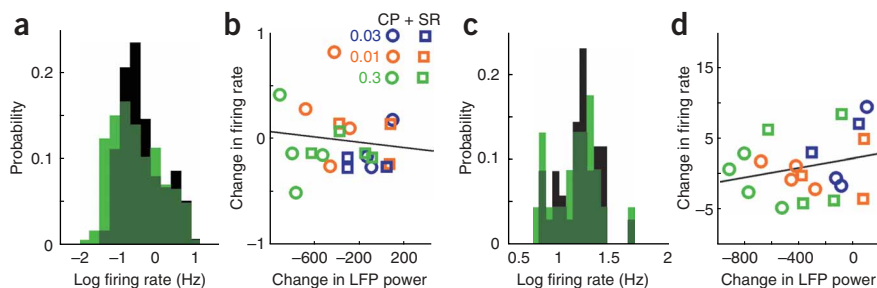
Figure 5 Cannabinoid-induced decrease of power cannot be explained by firing rate changes. (**a**) Mean firing rate distribution of pyramidal cells (control: $n = 316$, 4 rats, 8 experiments, population average is 1.08 Hz ± 0.10; CP55940: $n = 186$, 4 rats, 4 experiments, 1.00 Hz ± 0.12; $P = 0.005$). (**b**) Lack of correlation between LFP power change and shifts in firing rates of pyramidal cells across individual experiments. (**c**) Mean firing rate distribution of interneurons (control: $n = 35$, 18.15 Hz ± 0.52; CP55940: $n = 23$; 16.83 ± 0.78, $P = 0.41$). (**d**) Lack of correlation between changes in LFP power change and firing rates of interneurons across individual experiments.

areas not affected by the drug are likely to confound the field measures. Overall, these findings demonstrate that at least part of the CP55940 effects observed after systemic injection is mediated by intrahippocampal mechanisms.

Dissociation between changes in LFP power and firing rate

LFPs arise primarily from the extracellular summation of inhibitory and excitatory synaptic potentials[14]. The general depression of LFP may reflect a decreased synaptic activity associated with reduced firing rates, as observed with anesthetics[23]. Alternatively, cannabinoids may alter the temporal coordination of cell assemblies, the net result of which is the reduction of oscillatory patterns without major alterations in long-term mean firing rates. To address these hypotheses, we examined the effects of the CB1 agonist on the firing rates and discharge dynamics of isolated pyramidal cell and interneuron populations recorded in head-restrained rats. On average, 46 cells (range 7–90) were simultaneously recorded in each of these experiments from the pyramidal layer of the CA1 hippocampal region (**Supplementary Fig. 2** online). We found a small (7.4%), albeit significant, reduction in pyramidal cell discharge rates at the largest dose (**Fig. 5a**, 0.3 mg kg^{-1}; $P = 0.005$)[24]. However, this alone cannot account for the robust decrease in the oscillatory LFP because the direction and magnitude of firing rate changes did not correlate with the decreased LFP power in individual experiments (**Fig. 5b**, $r = -0.14$, $P = 0.54$). Similarly, the averaged firing rates of the interneuron population were not affected by the largest dose of CP55940 (**Fig. 5c**, $P = 0.41$) and changes in individual experiments did not correlate with LFP power alteration (**Fig. 5d**, $r = 0.25$, $P = 0.3$).
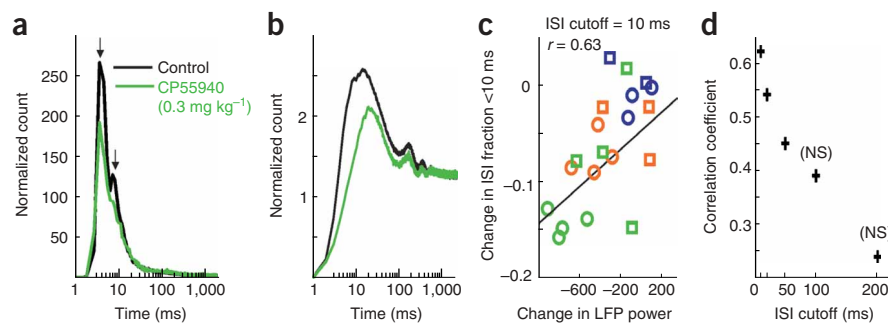
Cannabinoid disrupts firing patterns

In the intact hippocampus, pyramidal neurons discharge characteristic bursts of spikes at short (<6 ms) interspike intervals, when driven by synchronous inputs[25,26]. Interneurons do not have true bursts, nevertheless their firing patterns faithfully reflect the synchrony of the principal cell population and alternations in network behavior[26,27]. Both the burst

discharge of pyramidal cells (**Fig. 6a**) and the short-term firing patterns of interneurons (**Fig. 6b**), quantified by computing auto-correlograms, were profoundly affected by CP55940 (see also **Fig. 7a** and **Supplementary Figs. 3** and **4** online). Since interneuronal activity reflects population synchrony in a linear fashion[26,27] and CP55940 selectively decreased the incidence of short interspike intervals (ISIs, **Fig. 6b**), we examined the relationship between the change in short ISI incidence of interneurons and the change in LFP power. For each interneuron, we generated a single measure, the mean fraction of all ISIs that were shorter than 10 ms. For the interneuron population, the mean value of this measure in the control condition (0.22 ± 0.11 s.d.), was robustly decreased by 45% by CP55940 (0.12 ± 0.12 s.d.; $P < 0.001$). A comparison between the drug-induced change in this measure and the integral of the LFP power decrease between 1 and 200 Hz in individual experiments showed a significant positive correlation (**Fig. 6c**, $r = 0.63$, $P = 0.0025$), both demonstrating the receptor specificity of the effect and suggesting a role played by interneurons in the decrease of LFP power. To further examine the relationship between drug-induced changes in interneuron ISIs and LFP, we repeated this analysis using longer ISI cutoffs (20, 50, 100 and 200 ms, **Fig. 6d**). The correlation remained significant when the ISI cutoff was relaxed to 50 ms but not at longer intervals (for further quantification of spike time changes, see **Supplementary Figs. 3** and **4**).

CB1 receptor activation destroys assembly organization

Since the firing patterns but not the overall rates of both pyramidal cells and interneurons were affected by CP55940, we hypothesized that CB1 receptor activation impairs cell assembly coordination. Visual inspection of spike trains in the control condition or after CP55940 injection supported this suggestion (**Fig. 7a**). To quantify temporal synchrony, we computed cross-correlograms for all simultaneously recorded cell pairs. Following CP55940 injection, the temporal synchrony of cell

Figure 6 Cannabinoid-induced alteration of firing patterns of hippocampal cells. (**a**) Mean auto-correlogram of pyramidal cells (control, $n = 274$, 4 rats, 8 experiments; CP55940: $n = 133$, 4 rats, 4 experiments; integral values 4 to 17 ms: $P = 0.0067$). Positive part of auto-correlogram is shown to allow for log scale display. Arrows show burst peak at approximately 4 and 8 ms. (**b**) Similar display for interneurons (control, $n = 35$, 4 rats, 8 experiments; CP55940: $n = 23$, 4 rats, 4 experiments; integral values 4 to 50 ms: $P = 0.002$). (**c**) Correlation between LFP power and change in the mean fraction of interspike intervals (ISI) < 10 ms for interneurons. Same symbols as in **Figure 5**. (**d**) Correlation coefficients (same analysis as in **c**) for longer ISI cutoffs. Note that at longer ISI cutoffs, the correlation coefficients decrease ($P = 0.002$, 0.013, 0.043, 0.085, 0.25 for 10, 20, 50, 100 and 200 ms, respectively).
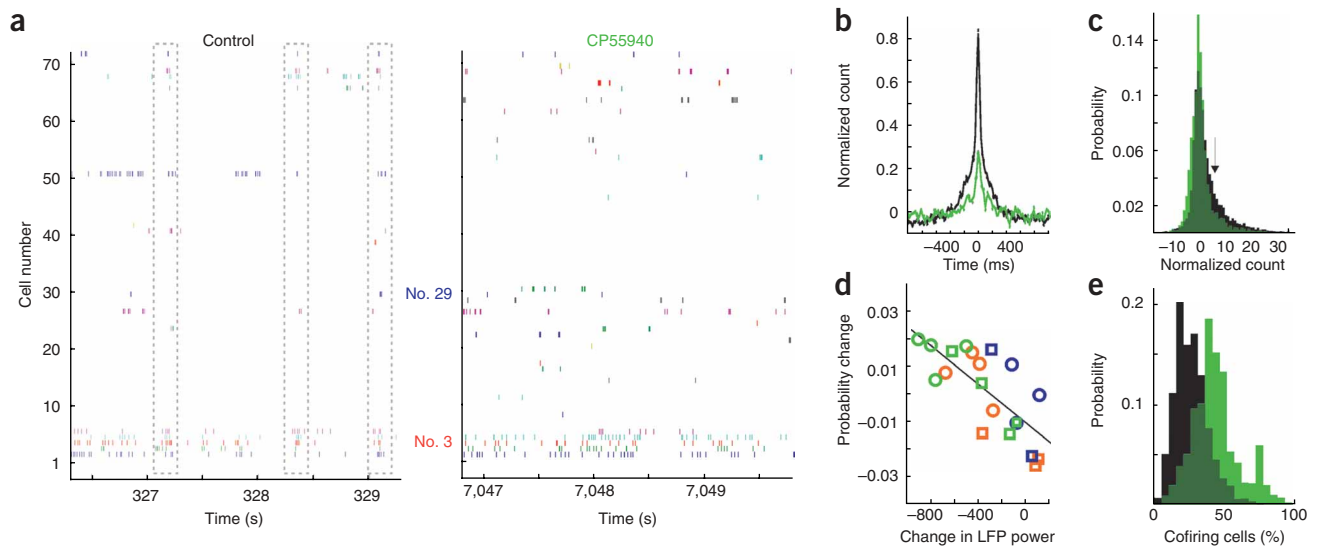
Figure 7 CP55940 destroys cell assembly organization. (**a**) Representative raster plots of 71 simultaneously recorded CA1 cells in control condition (left) and after 0.3 mg kg^{-1} CP55940 (right). Cells 1 to 5 are interneurons. Firing patterns of cells 3 and 29 are illustrated in **Supplementary Figure 4**. Twelve and 27 pyramidal cells fired at least one spike during the 3-s segments of the control (left) and drug (right) conditions. The total number of spikes in the population remained unaltered after the drug (271 versus 270 spikes). Framed areas show synchronous discharges. (**b**) Mean ± s.e.m. cross-correlograms from all recorded pairs (control: $n = 3,868$ pairs, 4 rats, 8 experiments; CP55940: $n = 1,777$ pairs, 4 rats, 4 experiments). (**c**) Distribution of cross-correlograms peak values before and after CP55940. (**d**) Correlation between LFP power and change in the distribution of cross-correlograms peak values (arrow in **c**) across individual experiments. Same symbols as in **Figure 5b**. (**e**) Distribution of the percentage of cofiring pyramidal cells in 3-s windows.

pairs was significantly reduced, as demonstrated by decreased spike coactivation in the central peak of the cross-correlograms (–100 to +100 ms; **Fig. 7b,c**; $P < 0.001$). Calculating the average change in the central bins of the distribution for all neuron pairs in each experiment and relating it to the drug-induced decrease in LFP power revealed a significant correlation (**Fig. 7d**; $r = -0.73$, $P < 0.001$), demonstrating that the observed decrease in LFP power is associated with decreased neuronal synchrony; this also showed the receptor specificity of the effect. In another comparison, we examined the percentage of coactive cells in longer time windows (3 s), excluding ripple events. Under the influence of CP55940, the number of cells active (i.e., firing at least one spike) over such long intervals significantly increased (**Fig. 7e**; $P < 0.001$).

The correlation analyses performed across experiments support the role of population synchrony over firing rates in LFP production. However, because these analyses were performed on data from the whole recording session, they do not rule out the possibility that changes in firing rate and/or synchrony during nontheta/nonripple (flat) network states biased the results. LFP power decreased substantially after cannabinoid administration, making the identification of theta and ripple epochs for separate analysis implausible. Therefore, we took a conservative approach to rule out the contribution of firing rate

changes during nontheta/nonripple epochs by performing separate analyses on identified flat LFP epochs. The power distribution of spectra derived from the flat epochs in control and drug sessions were indistinguishable (**Fig. 8a**). In addition, the average firing rates of pyramidal cells and interneurons associated with the flat LFP epochs were comparable (**Fig. 8b,c**). The firing patterns of pyramidal cells in control sessions were characterized by a bimodal distribution of discharge rates, with most neurons discharging at a very low rate, while a small minority fired between 5 and 15 Hz. In contrast, the distribution became unimodal after CP55940 application, with most
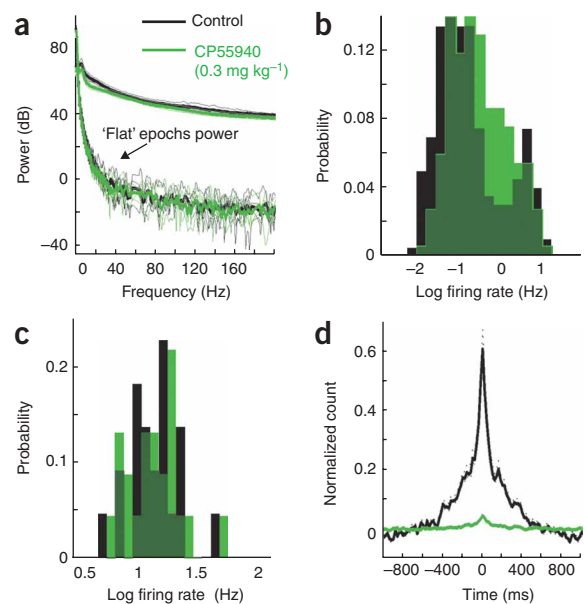
Figure 8 During 'flat' LFP epochs, CP55940 decreases spike synchrony while preserving average firing rates. (**a**) LFP power of flat epochs (no theta and no ripple oscillations). (**b**) Distribution of pyramidal cell firing rates (control: $n = 202$, 4 rats, 4 experiments, population average is 0.95 Hz ± 0.14; CP55940: $n = 187$, 4 rats, 4 experiments, 0.94 Hz ± 0.12; $P < 0.001$). (**c**) Distribution of interneuron firing rates (control: $n = 23$, 4 rats, 4 experiments, 15.64 Hz ± 0.61; CP55940: $n = 22$, 4 rats, 4 experiments, 15.81 ± 0.76; $P = 0.94$). (**d**) Group mean cross-correlograms of neuron pairs (control: $n = 1,129$ pairs, 4 rats, 4 experiments; CP55940: $n = 2,899$ pairs, $P < 0.001$ at the peak value; mean ± s.e.m.).

cells discharging less than 0.5 Hz (**Fig. 8b**, $P < 0.001$). As illustrated in **Figure 7a**, the most dramatic effect of the drug was the decrease in neuronal synchrony, as demonstrated by the virtual absence of spike coactivation (**Fig. 8d**; $P < 0.001$).

DISCUSSION

Our findings demonstrate that cannabinoids, at doses comparable with recreational[4] and palliative[28] uses in humans, reduce assembly synchrony in the hippocampus while preserving the firing rates of individual neurons. We hypothesize that the lack of proper temporal coordination among neurons is the immediate cause for the cannabinoid-induced impairment of hippocampus-dependent memory[7–9] (and present study). Since the changes in LFP power correlated with changes in population synchrony rather than firing rate alterations, our data also support the importance of spike timing in physiological functions of the hippocampus.

Effects of cannabinoids on oscillations and behavior

Theta and associated gamma LFP oscillations occur during exploratory behavior and rapid eye movement sleep, whereas sharp wave associated ripples are observed during slow wave sleep, immobility and consummatory behavior[18]. It has been hypothesized that theta/gamma oscillations are involved in memory encoding and plasticity, whereas the fast ripple oscillations are critical for the transfer of information from the hippocampus to the neocortex[18,19]. Previous investigations have reported that cannabinoids decrease hippocampal LFP power in the theta and gamma bands[11,12]. In those studies, however, the effects of the drug on overt aspects of behavior and physiological parameters could not be dissociated. In our study, several observations argue against a simple, overt behavior-mediated effect on these oscillatory patterns following CB1 receptor activation. While cannabinoids are known to increase immobility[2], both ripples and theta power were suppressed by cannabinoids in head-restrained, freely behaving and anesthetized rats. This indicates that CP55940 did not simply shift behavior or the network state of the hippocampus from theta to nontheta mode. Additionally, the decrease in theta oscillations observed in awake animals cannot be fully explained by decreased locomotion because a significant reduction in theta power was observed at comparable running speeds before and after cannabinoid treatment. On the other hand, because the speed-independent decrease in theta power brought about by CP55940 was correlated with memory impairment in the delayed spatial alternation task, our data support the hypothesis that cannabinoid-induced disruption of hippocampal oscillatory patterns is related to hippocampal dysfunction.

Cannabinoids could potentially impair hippocampus-dependent behaviors by extra-hippocampal mechanisms, including modulation of the subcortical neurotransmitters acetylcholine, serotonin and dopamine[29–31]. Although theta oscillations are promoted by subcortical neuromodulators[32], ripples can occur in their absence[18,33]. Thus, the simultaneous decrease of theta, gamma and ripple oscillations by cannabinoids cannot simply be explained by a global change in neuromodulation and brain state changes. Furthermore, gamma oscillations induced by kainic acid in the CA3 region of hippocampal slices are dramatically reduced by the CB1 receptor agonist CP55940 (ref. 13), suggesting that cannabinoids can directly affect hippocampal network activity *in vivo*. Finally, intrahippocampal injections of the CB1 receptor agonist CP55940 also reduced the incidence and power of locally generated ripples. Although our findings do not conclusively exclude the contribution of extrahippocampal factors, they point to mechanisms by which cannabinoids disrupt hippocampal network patterns and hippocampus-dependent memory in both experimental and recreational settings.

Mechanisms for the disruption of hippocampal oscillations

Because performance of hippocampus-dependent tasks is severely disrupted by both systemic and local administration of cannabinoids[7–9], we investigated the impact of cannabinoids on hippocampal network activity. The most striking observation of our study is that cannabinoids disrupt the organization of cell assemblies without substantially affecting the average firing rates of neurons. Whereas the balance between excitatory and inhibitory firing rates was marginally affected by cannabinoids at the time-scale of seconds, the fine time-scale temporal patterns of neuronal discharges were robustly affected at both single cell and population levels. At the single cell level, this was reflected by reduced burstiness of pyramidal neurons and decreased probability of short interval spikes in interneurons. The impairment of temporal coordination was even more striking at the population level. Synchrony of neurons at the time scales of network oscillation patterns was severely reduced by the drug. At the same time, more neurons were active, albeit at a low rate, in larger time windows.

Previous work[13] suggested that the decrease of kainate-induced gamma oscillations by CP55940 is due to a reduction of inhibitory postsynaptic potentials (IPSPs), presumably mediated by CCK-immunoreactive interneurons. However, cannabinoid activation of CB1 receptors located on the terminals of CCK-immunoreactive neurons alone cannot explain the present findings, because the reduction of GABAergic inhibition is expected to increase excitability in the network. Instead, we found decreased excitability without major changes in firing rates, suggesting that the excitatory interactions of the principal cells were also affected. First, burst discharges of hippocampal pyramidal neurons require synchronous convergent excitation[26], and the incidence of bursts was significantly reduced by cannabinoids. Second, sharp wave-ripple complexes are generated through the synchronous discharge of CA3 pyramidal cells converging on CA1 pyramidal cells and interneurons[21], and ripple power was dramatically reduced. Altered GABA release from CCK interneurons likely does not contribute significantly to this effect, since CCK interneurons are silent during ripples[34]. Finally, theta and gamma oscillations depend on both excitatory and inhibitory synaptic transmission[35–37], and their power was also decreased by cannabinoids. These findings provide physiological support for the recently documented expression of CB1 receptors on synaptic terminals of principal cells in the hippocampus[38–40].

Reduced transmitter release from glutamatergic terminals may be the primary factor in the network effects of cannabinoids. Decreased excitation of principal cells reduces their excitability and consequently the excitatory drive of interneurons, even if the pyramidal cell-interneuron synaptic transmission is not affected by cannabinoids[41]. Furthermore, spike 'doublets' in interneurons have been shown to reflect synchronization of spatially distant gamma oscillators[42]. In light of the doublets mechanism, the reduction of spike bursts in interneurons, due to reduced drive from both local and distant asynchronously discharging pyramidal cells, can contribute to the reduction of oscillation power. We propose that reduced neuronal synchrony is the immediate cause of the large drug-induced decrease in the power of field oscillations, a hypothesis supported by the correlation between synchronous discharge of neurons and the magnitude of LFP power. Although modification of oscillatory patterns is often observed after surgical and pharmacological interference in the medial septum[43,44] and systemic treatment with anesthetics[23] or $GABA_B$ agonists[45], alteration of LFP power independent of firing rates changes appears

to be a unique effect of CB1 agonists. This may be brought about by a balanced decrease in glutamate release from excitatory afferents, reduction in GABAergic inhibition by CCK interneurons and the indirect reduced excitatory drive of other interneurons[1,38,39,41].

Overall, our findings indicate that under the influence of cannabinoids, neurons are liberated from population control. Although individual neurons continue to discharge at the same rate, they fail to organize into temporally coordinated assemblies. A clear disadvantage of decreased synchrony is the reduced effectiveness of the population output on their downstream targets, even though the same numbers of spikes are emitted[46]. We hypothesize that such hippocampus-wide impairment of network coordination, reflected by the reduction of LFP power, is causally related to the cannabinoid-induced memory impairment. The synchrony-reducing effects of CB1 receptor activation may also underlie the antiepileptic effects of endocannabinoids[47–49].

METHODS

Recording protocols and data acquisition. Silicon probes and tetrodes were used to record multiple single units and LFP from head-restrained ($n = 4$) and freely moving ($n = 7$) rats (see **Supplementary Methods** for details on training and recording procedures). In addition, for local injection experiments, tungsten wires were used to record LFP from urethane-anesthetized rats ($n = 3$, see **Supplementary Methods**). All protocols were approved by the Institutional Animal Care and Use Committee of Rutgers University.

During the recording sessions, neurophysiological signals were acquired continuously at 20 kHz on either a 64-channel DataMax system (16-bit resolution; RC Electronics) or a 64-Channel Cheetah System (Unit, 32 kHz, LFP 2.6 kHz, 24-bit resolution, Neuralynx). For offline spike sorting, the wide-band signals were digitally high-pass filtered (0.8–5 kHz). For tracking the position of the animals on the elevated track, two small light-emitting diodes (5-cm separation), mounted above the headstage, were recorded by a digital video camera and sampled at 40 Hz or 60 Hz. Neurophysiological and behavioral data were explored using NeuroScope (see URLs)[50]. Spike sorting was performed automatically, using KlustaKwik (see URLs), followed by manual adjustment of the clusters (using the Klusters software package; see URLs)[50]. Pyramidal cells and interneurons were separated on the basis of their auto-correlograms, waveforms and mean firing rate (**Supplementary Fig. 1**)[21]. Neurons that did not fit these criteria were excluded from further analysis. Only units with clear refractory periods and well-defined cluster boundaries were included in the analysis. Spike sorting was performed blindly and independently for each drug condition.

Data analysis. Data analysis was carried out by custom-written Matlab-based software (Mathworks). For each head-restrained experiment, LFP power analysis was performed on the shank displaying the largest ripples, indicating the middle of the CA1 pyramidal layer. LFP data were extracted from four neighboring recording sites and averaged. Calculation of power spectral density analysis was performed on the averaged LFP using the multi-taper estimates method. For comparison of power spectra and unit activity, the full recording, starting 20 min after the vehicle or drug injection were used. Ripples were detected by filtering the average LFP (100–200 Hz). The filtered signal was standardized ((signal − mean(signal)/std(signal)) and events exceeding 4 s.d. were detected and classified as ripples. All detected oscillations (ripples and theta) were visually inspected, superimposed on the raw traces and adjusted manually, if necessary.

For local injection experiments, ripples epochs were detected from electrode 4 of the vehicle-injected side (inset of **Fig. 4a**) and served as a reference to calculate of ripple power ratios for each electrode for all events.

Cross-correlograms were normalized by the asymptotic mean firing rates of both spike trains to obtain a correlation index (*c.i.*). A *c.i.* of 1 corresponds to independent firing, *c.i.* values less than 1 indicate explicitly uncorrelated firing and *c.i.* values greater than 1 indicate correlated firing. To eliminate the contribution of slow time scale (>1 s) synchrony brought about by state changes, spike trains were randomly shuffled using a ± 1 s time jitter. The shuffled cross-correlograms (which contained only slow time scale correlations)

were then subtracted from the original. The difference cross-correlogram accounts only for fast (<1 s) spike interactions (**Figs. 7b** and **8f**).

For behavioral experiments, independent measurements of power spectra and running speed were calculated using 1-s nonoverlapping windows. The center-weighted average of the running speed in each window was calculated by convolving with a normalized Hanning window. Analysis of covariance tests were performed to examine the drug effect on theta power while controlling for relationship between running speed and theta power. Windows with average speed less than 1 cm s^{-1} were removed from the theta power analysis to eliminate the contribution of immobility periods to theta power estimates. To assess the change in theta power between control and drug conditions independent of changes in running speed, the control and CP55940 speed/power relationship were regressed for the two groups using parallel fits (broken lines, **Fig. 2b**). The distance between these two fits (arrow in **Fig. 2b**) represents the decrease in theta power brought by CP55940, independently of any changes in speed.

Statistical comparisons included ranksum tests (nonparametric data), one- and two-way ANOVA tests (parametric data), Kolmogorov-Smirnov and ANCOVA tests.

Drugs and injections. CP55940 was obtained from Tocris or Sigma and SR141716A was a courtesy gift from the US National Institutes of Health (NIH). For systemic injections, stock solutions of CP55940 and SR141716A were prepared in ethanol at a concentration of 3 and 15 mg ml^{-1}, respectively. The injected solutions were a mixture of 10% stock solution, 10% Cremaphor (Sigma) and 80% saline. The volume of injection was of 0.1 ml per 100 g of body weight. Control injections were performed with the vehicle alone. For the head-restrained experiments, two recording sessions were performed in each animal, separated by an interval of at least 72 h. Recordings started 20 min after each injection. Vehicle alone had no effect on LFP power or firing rates or behavioral performance (data not shown). Δ^9-THC was obtained from Sigma and dissolved in a solution of 20% DMSO, 10% Tween-80 and 70% saline, for final concentrations of 5 mg kg^{-1}. LFP oscillations returned to normal levels the day following the experiments.

URLs. Neuroscope, http://neuroscope.sourceforge.net. KlustaKwik, http://sourceforge.net/projects/klustakwik. Klusters, http://sourceforge.net/projects/klusters.

Note: Supplementary information is available on the Nature Neuroscience website.

AUTHOR CONTRIBUTIONS
D.R. conducted the recordings in head-restrained, anesthetized and freely moving ($n = 3$) rats and did most of the data analysis. S.M.M. conducted recordings in freely moving rats ($n = 2$) and designed the covariance analysis test. P.E.R.-O. participated in the recordings of two freely moving rats. A.T. conducted and B.L.M. supervised the Δ^9-THC experiments. G.B. supervised the project and cowrote the manuscript with D.R. and S.M.M.

COMPETING INTERESTS STATEMENT
The authors declare that they have no competing financial interests.

1. Freund, T.F., Katona, I. & Piomelli, D. Role of endogenous cannabinoids in synaptic signaling. *Physiol. Rev.* **83**, 1017–1066 (2003).
2. Ameri, A. The effects of cannabinoids on the brain. *Prog. Neurobiol.* **58**, 315–348 (1999).
3. Ilan, A.B., Smith, M.E. & Gevins, A. Effects of marijuana on neurophysiological signals of working and episodic memory. *Psychopharmacology (Berl.)* **176**, 214–222 (2004).
4. Curran, H.V., Brignell, C., Fletcher, S., Middleton, P. & Henry, J. Cognitive and subjective dose-response effects of acute oral delta 9-tetrahydrocannabinol (THC) in infrequent cannabis users. *Psychopharmacology (Berl.)* **164**, 61–70 (2002).

5. Miller, L.L. & Branconnier, R.J. Cannabis: effects on memory and the cholinergic limbic system. *Psychol. Bull.* **93**, 441–456 (1983).
6. Squire, L.R., Stark, C.E. & Clark, R.E. The medial temporal lobe. *Annu. Rev. Neurosci.* **27**, 279–306 (2004).
7. Lichtman, A.H. & Martin, B.R. Delta 9-tetrahydrocannabinol impairs spatial memory through a cannabinoid receptor mechanism. *Psychopharmacology (Berl.)* **126**, 125–131 (1996).
8. Lichtman, A.H., Dimen, K.R. & Martin, B.R. Systemic or intrahippocampal cannabinoid administration impairs spatial memory in rats. *Psychopharmacology (Berl.)* **119**, 282–290 (1995).
9. Hampson, R.E. & Deadwyler, S.A. Role of cannabinoid receptors in memory storage. *Neurobiol. Dis.* **5**, 474–482 (1998).
10. Buonamici, M., Young, G.A. & Khazan, N. Effects of acute delta 9-THC administration on EEG and EEG power spectra in the rat. *Neuropharmacology* **21**, 825–829 (1982).
11. Constoe, P.F., Jones, B.C. & Chin, L. Delta-9-tetrahydrocannabinol, EEG and behavior:the importance of adaptation to the testing milieu. *Pharmacol. Biochem. Behav.* **3**, 173–177 (1975).
12. Willinsky, M.D., Loizzo, A. & Longo, V.G. EEG spectral analysis for the evaluation of the central effects of delta6-tetrahydrocannabinol in rabbits. *Psychopharmacologia* **41**, 123–126 (1975).
13. Hajos, N. *et al.* Cannabinoids inhibit hippocampal GABAergic transmission and network oscillations. *Eur. J. Neurosci.* **12**, 3239–3249 (2000).
14. Buzsáki, G., Traub, R.D. & Pedley, T. The cellular synaptic generation of EEG. in *Current Practice of Clinical Encephalography* (eds. J.S. Ebersole and T.A. Pedley) 1–11 (Lippincott-Williams and Wilkins, Philadelphia, 2003).
15. Siapas, A.G., Lubenov, E.V. & Wilson, M.A. Prefrontal phase locking to hippocampal theta oscillations. *Neuron* **46**, 141–151 (2005).
16. Lee, H., Simpson, G.V., Logothetis, N.K. & Rainer, G. Phase locking of single neuron activity to theta oscillations during working memory in monkey extrastriate visual cortex. *Neuron* **45**, 147–156 (2005).
17. Hasselmo, M.E., Bodelon, C. & Wyble, B.P. A proposed function for hippocampal theta rhythm: separate phases of encoding and retrieval enhance reversal of prior learning. *Neural Comput.* **14**, 793–817 (2002).
18. Buzsaki, G. The hippocampo-neocortical dialogue. *Cereb. Cortex* **6**, 81–92 (1996).
19. Kudrimoti, H.S., Barnes, C.A. & McNaughton, B.L. Reactivation of hippocampal cell assemblies: effects of behavioral state, experience and EEG dynamics. *J. Neurosci.* **19**, 4090–4101 (1999).
20. Chrobak, J.J. & Buzsaki, G. High-frequency oscillations in the output networks of the hippocampal-entorhinal axis of the freely behaving rat. *J. Neurosci.* **16**, 3056–3066 (1996).
21. Csicsvari, J., Hirase, H., Mamiya, A. & Buzsaki, G. Ensemble patterns of hippocampal CA3-CA1 neurons during sharp wave-associated population events. *Neuron* **28**, 585–594 (2000).
22. Nunez, P.L. *et al.* EEG coherency. I: Statistics, reference electrode, volume conduction, Laplacians, cortical imaging, and interpretation at multiple scales. *Electroencephalogr. Clin. Neurophysiol.* **103**, 499–515 (1997).
23. Destexhe, A., Rudolph, M. & Pare, D. The high-conductance state of neocortical neurons *in vivo. Nat. Rev. Neurosci.* **4**, 739–751 (2003).
24. Hampson, R.E. & Deadwyler, S.A. Cannabinoids reveal the necessity of hippocampal neural encoding for short-term memory in rats. *J. Neurosci.* **20**, 8932–8942 (2000).
25. Lisman, J.E. Bursts as a unit of neural information: making unreliable synapses reliable. *Trends Neurosci.* **20**, 38–43 (1997).
26. Harris, K.D., Hirase, H., Leinekugel, X., Henze, D.A. & Buzsaki, G. Temporal interaction between single spikes and complex spike bursts in hippocampal pyramidal cells. *Neuron* **32**, 141–149 (2001).
27. Freund, T.F. & Buzsaki, G. Interneurons of the hippocampus. *Hippocampus.* **6**, 347–470 (1996).
28. Robson, P. Therapeutic aspects of cannabis and cannabinoids. *Br. J. Psychiatry.* **178**, 107–115 (2001).
29. Pisanu, A., Acquas, E., Fenu, S. & Di Chiara, G. Modulation of Δ^9-THC-induced increase of cortical and hippocampal acetylcholine release by μ opioid and D_1 dopamine receptors. *Neuropharmacology* **50**, 661–670 (2006).
30. Tzavara, E.T., Wade, M. & Nomikos, G.G. Biphasic effects of cannabinoids on acetylcholine release in the hippocampus: site and mechanism of action. *J. Neurosci.* **23**, 9374–9384 (2003).
31. Egashira, N. *et al.* Involvement of 5-hydroxytryptamine neuronal system in Δ^9-tetrahydrocannabinol-induced impairment of spatial memory. *Eur. J. Pharmacol.* **445**, 221–229 (2002).
32. Bland, B.H. The physiology and pharmacology of hippocampal formation theta rhythms. *Prog. Neurobiol.* **26**, 1–54 (1986).
33. Behrens, C.J., van den Boom, L.P., de, H.L., Friedman, A. & Heinemann, U. Induction of sharp wave-ripple complexes *in vitro* and reorganization of hippocampal networks. *Nat. Neurosci.* **8**, 1560–1567 (2005).
34. Klausberger, T. *et al.* Complementary roles of cholecystokinin- and parvalbumin-expressing GABAergic neurons in hippocampal network oscillations. *J. Neurosci.* **25**, 9782–9793 (2005).
35. Csicsvari, J., Jamieson, B., Wise, K.D. & Buzsaki, G. Mechanisms of gamma oscillations in the hippocampus of the behaving rat. *Neuron.* **37**, 311–322 (2003).
36. Fisahn, A., Pike, F.G., Buhl, E.H. & Paulsen, O. Cholinergic induction of network oscillations at 40 Hz in the hippocampus *in vitro. Nature.* **394**, 186–189 (1998).
37. Buzsaki, G. Theta oscillations in the hippocampus. *Neuron.* **33**, 325–340 (2002).
38. Kawamura, Y. *et al.* The CB1 cannabinoid receptor is the major cannabinoid receptor at excitatory presynaptic sites in the hippocampus and cerebellum. *J. Neurosci.* **26**, 2991–3001 (2006).
39. Takahashi, K.A. & Castillo, P.E. The CB1 cannabinoid receptor mediates glutamatergic synaptic suppression in the hippocampus. *Neuroscience* **139**, 795–802 (2006).
40. Katona, I. *et al.* Molecular composition of the endocannabinoid system at glutamatergic synapses. *J. Neurosci.* **26**, 5628–5637 (2006).
41. Hoffman, A.F., Riegel, A.C. & Lupica, C.R. Functional localization of cannabinoid receptors and endogenous cannabinoid production in distinct neuron populations of the hippocampus. *Eur. J. Neurosci.* **18**, 524–534 (2003).
42. Traub, R.D., Whittington, M.A., Stanford, I.M. & Jefferys, J.G. A mechanism for generation of long-range synchronous fast oscillations in the cortex. *Nature* **383**, 621–624 (1996).
43. Givens, B.S. & Olton, D.S. Cholinergic and GABAergic modulation of medial septal area: effect on working memory. *Behav. Neurosci.* **104**, 849–855 (1990).
44. Mizumori, S.J., Perez, G.M., Alvarado, M.C., Barnes, C.A. & McNaughton, B.L. Reversible inactivation of the medial septum differentially affects two forms of learning in rats. *Brain Res.* **528**, 12–20 (1990).
45. Olpe, H.-R., Glatt, A. & Bencze, W. Electrophysiological manifestations of supraspinal actions of baclofen. *Brain Res. Bull.* **5**, 507–511 (1980).
46. Konig, P., Engel, A.K. & Singer, W. Integrator or coincidence detector? The role of the cortical neuron revisited. *Trends Neurosci.* **19**, 130–137 (1996).
47. Monory, K. *et al.* The endocannabinoid system controls key epileptogenic circuits in the hippocampus. *Neuron* **51**, 455–466 (2006).
48. Marsicano, G. *et al.* CB1 cannabinoid receptors and on-demand defense against excitotoxicity. *Science* **302**, 84–88 (2003).
49. Bernard, C. *et al.* Altering cannabinoid signaling during development disrupts neuronal activity. *Proc. Natl. Acad. Sci. USA* **102**, 9388–9393 (2005).
50. Hazan, L., Zugaro, M. & Buzsaki, G. Klusters, NeuroScope, NDManager: a free software suite for neurophysiological data processing and visualization. *J. Neurosci. Methods* **155**, 207–216 (2006).